PAGEOPH, Vol. 146, No. 2 (1996)

0033–4553/96/020229–24$1.50 + 0.20/0

Evolution of Localized Folding for a Thin Elastic Layer in a Softening Visco-elastic Medium

G. W. HUNT,[1] H-B. MÜHLHAUS[2] and A. I. M. WHITING[1]

Abstract—Long compressed elastic struts on softening elastic foundations have a tendency to buckle locally. The same tendency is demonstrated here for the instantaneous response of elastic struts supported by visco-elastic media. A governing nonlinear partial differential equation is derived to describe the evolution of the localized form in time. Under the assumed constant end-shortening this is found to be approximated by a coupled set of seven ordinary differential (diffusion) equations. As the load drops to zero, the localized buckle pattern evolves towards the form of the single long wave, but remains aperiodic for all time. Three-dimensional plots show how this localized pattern changes over time.

Key words: Localized folding, softening visco-elastic medium, instability of layer.

1. Introduction

It is commonly held amongst structural geologists that the folding of stratified rock is a slow process, and therefore is primarily a controlled viscous phenomenon. There is however a growing realization, succinctly put by PRICE and COSGROVE (1990) for example at the end of the chapter entitled "Introduction to Folding," that much of what is observed may be due to inherent elasticity. In referring to the viscous studies of BIOT (1965) and others, they comment ". . . their predicted results regarding L/a ratios have not fitted observed natural data. Only by treating rocks as highly nonlinear viscous materials has it proved possible to bring theory and field observations into line. This problem has arisen because it has been implicitly assumed that elastic behaviour of rocks during the initiation of folding can be ignored" (after PRICE and COSGROVE, 1990). The present paper shows one effect of introducing nonlinearity into the bedding relations, for a thin strip of elastic material supported within a visco-elastic (Maxwell) medium.

We find that elasticity in the embedding medium provides the opportunity for "instantaneous" elastic behaviour to affect the form of deformation before viscosity

[1] Department of Civil Engineering, Imperial College London, UK.
[2] Division of Exploration and Mining, CSIRO, Perth, Australia.

and consequent dissipation have had time to play their part. Not only are wavelengths (L/a ratios) affected, but new structural forms can emerge; the opening exists for some of the rich and varied bifurcation phenomena of elastic buckling to appear at the start of the evolutionary process, with continuing influences as time progresses. The response of the system, in a time scale associated with the rate of loading, mirrors that of pure elasticity, yet in the longer time scale the response is effectively governed by the viscous part of the embedding medium. What is unstable in the sense of the latter may be stable in the sense of the former, and both elastic and viscous parts are germane to what may be seen.

In particular, with a softening nonlinearity in the bedding relation, the system settles naturally at the start of evolution into a pattern of localized buckling, contrasting sharply with the strongly-periodic trend found in purely viscous formulations (BIOT, 1965; MÜHLHAUS *et al.*, 1994). Localized buckling has a wide range of spectacular variations, with a chaotic tendency that is only now being understood in the purely elastic case (HUNT and WADEE, 1991; CHAMPNEYS and TOLAND, 1993). Although the Maxwell representation of the bed is fundamentally that of a fluid, governed in the long term by viscosity, it is seen that for the limiting case of infinite length, the route to the fully relaxed state from an initial localization remains inherently aperiodic; periodicity, so dominant for purely viscous embedding, never makes an appearance. Thus localized forms are seen to be an integral part of the geological timeframe.

2. Linear Fourier Analysis

We start with the small displacement response of an incompressible elastic layer of length L, thickness h and shear modulus G, embedded in a medium of vertical resistance per unit length, q, and compressed horizontally by an axial load P. This is describable by the linear differential equation (BIOT, 1965),

$$\frac{Gh^3}{3}\partial_x^4(w) + P\partial_x^2(w) - q = 0, \tag{1}$$

where ∂_x^i denotes i differentiations with respect to the spatial variable x. Deflections are taken as having no variation in the second horizontal dimension. The lateral deflection w is expressed as an infinite set of Fourier components with amplitudes a_m,

$$w = \sum_{m=0}^{\infty} w_m = \sum_{m=0}^{\infty} a_m \cos k_m x, \tag{2}$$

and we correspondingly define components of the bedding force,

$$q = \sum_{m=0}^{\infty} q_m \cos k_m x, \tag{3}$$

where $k_m = 2\pi m/L$, leading to the following relations in terms of the amplitudes a_m,

$$\frac{Gh^3}{3} k_m^4 a_m - P k_m^2 a_m - q_m = 0. \tag{4}$$

2.1. Elastic Bed

Let us suppose that the embedding medium extends to infinity in all directions, and initially is elastic. Following BIOT (1965), the amplitudes of the bedding force are related to the amplitudes of the buckle pattern by,

$$q_m = -4G_1 k_m a_m, \tag{5}$$

where G_1 is the bedding shear modulus. We note the wavelength dependence of this bedding relation (BIOT, 1965). After substituting into equation (4), we can write,

$$P = \frac{4G_1}{k_m} + \frac{Gh^3}{3} k_m^2, \tag{6}$$

and see that each wavenumber m has associated with it a different distinct critical load, P_m^C. If an elastic Winkler foundation instead of an infinite domain is used, the denominator of the first term appears as k_m^2 (HUNT and WADEE, 1991). Differentiating the expression for P with respect to k_m gives the minimum critical load and corresponding mode,

$$P_{\min}^C = \frac{6}{k_{\min}} G_1, \quad \text{where} \quad k_{\min} = \frac{1}{h} \sqrt[3]{\frac{6G_1}{G}}. \tag{7}$$

There is more than one way of nondimensionalizing the basic equation (1), depending on the characteristics of the bedding relation. For the present elastic system for example, we can introduce a nondimensional load $p = P/P_{\min}^C$, a nondimensional spatial measure $\tilde{x} = k_{\min} x$, and a "nondimensional" wavenumber $\tilde{k}_m = k_m/k_{\min}$, such that a "modal" form of equation (1) associated specifically with this wavenumber can be written.

$$w_m'''' + 3p w_m'' + 2\tilde{k}_m w_m = 0, \tag{8}$$

where a prime denotes differentiation with respect to $\tilde{x}$. We shall compare and contrast this with a second nondimensionalization, associated with the viscous properties of a visco-elastic bed, later in Section 2.3.

2.2 Viscous Bed

Again following BIOT (1965), we now presume the supporting medium is purely viscous, and write the amplitudes of the bedding force q as,

$$q_m = -4\eta_1 k_m \partial_t(a_m), \tag{9}$$

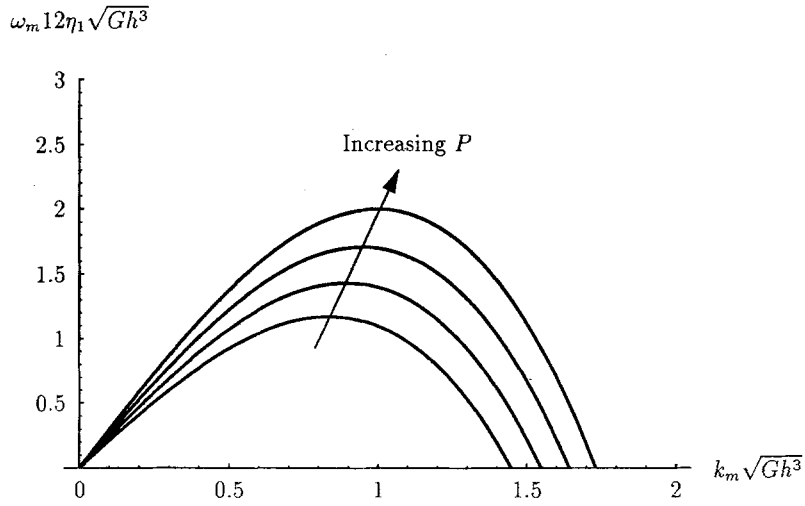

Figure 1
Dispersion relation for a purely viscous medium.

where η_1 is the bedding viscosity, and ∂_t denotes partial differentiation with respect to time t. We note again the dependence on wavenumber k_m. Substituting into equation (4) then gives,

$$\frac{Gh^3}{3}k_m^3 a_m - Pk_m a_m + 4\eta_1 \partial_t(a_m) = 0, \tag{10}$$

and adopting the eigenmode solution $a_m = A_m\, e^{\omega_m t}$ we obtain,

$$\frac{Gh^3}{3}k_m^3 - Pk_m + 4\eta_1\omega_m = 0, \tag{11}$$

leading to the *dispersion relation* for ω_m,

$$\omega_m = \frac{3Pk_m - Gh^3k_m^3}{12\eta_1}. \tag{12}$$

This suggests a quite different behaviour from that of the elastic system. Under constant load, at time t all wavelengths apart from that for $m = 0$ have a nontrivial form in x. Plotting ω_m against k_m gives the curves of Figure 1, with the dominant wavelength of BIOT (1965), corresponding to the most rapidly-growing amplitude, appearing when ω_m is a maximum. This is found simply by setting $d\omega_m/dk_m = 0$, to give,

$$\omega_d = \frac{P}{6\eta_1}k_d \quad \text{where} \quad k_d = \frac{1}{h}\sqrt{\frac{P}{Gh}}. \tag{13}$$

A different form of nondimensionalization is appropriate for a purely viscous bed. If we define a nondimensional spatial measure $\tilde{x} = k_d x$ and nondimensional time $\tilde{t} = \omega_d t$ with respect to the dominant viscous wavelength k_d, the following equation appears in the modal deflection function w_m,

$$w_m'''' + 3w_m'' + 2\tilde{k}_m \dot{w}_m = 0. \tag{14}$$

Here $\tilde{k}_m = k_m/k_d$, primes denote differentiation with respect to the new $\tilde{x}$ and a dot denotes differentiation with respect to $\tilde{t}$. We note the P-dependence of the transformations, but the absence of parametric variation with P from the final equation. However, if applied end-shortening rather than load is held constant, as in the work that follows, P varies over time, and the new spatial measure $\tilde{x}$, being P-dependent, must also change. To avoid this added complication, the P-independent nondimensionalization of the previous section is used exclusively in the nonlinear analysis.

2.3 Visco-elastic Bed

For a visco-elastic supporting medium under a harmonic deflection function $w_m(x)$, we write initially a strain rate equation for a bedding material with a Maxwell constitutive law in terms of amplitudes,

$$-4k_m \partial_t(a_m) = \frac{1}{G_1}\partial_t(q_m) + \frac{1}{\eta_1} q_m. \tag{15}$$

Operating symbolically we can then write,

$$q_m = -4G_1 k_m \left(\frac{\partial_t}{\partial_t + r}\right) a_m, \tag{16}$$

where $r = G_1/\eta_1$.

For a visco-elastic bed there is a choice of possible nondimensionalizations. Remembering the nondimensional load is defined by $p = P/P^C_{\min}$, we can take $\tilde{x} = k_{\min} x$ and $\tilde{k}_m = k_m/k_{\min}$ as with the elastic analysis, and introduce a related nondimensional time $\tilde{t} = rt$. Equation (1) now becomes,

$$\dot{w}_m'''' + 3p\dot{w}_m'' + 2\tilde{k}_m \dot{w}_m + w_m'''' + 3w_m''(p + \dot{p}) = 0. \tag{17}$$

Under constant load ($\dot{p} = 0$), with an assumed periodicity in x and the same eigensolution as before, $a_m = A_m \, e^{\tilde{\omega}_m \tilde{t}}$, after slight manipulation this gives a nondimensionalized visco-elastic dispersion relation,

$$\tilde{\omega}_m = \frac{3p\tilde{k}_m - \tilde{k}_m^3}{\tilde{k}_m^3 - 3p\tilde{k}_m + 2}. \tag{18}$$

Plotting $\tilde{\omega}_m$ against $\tilde{k}_m$ then creates the family of curves shown in Figure 2(a). As p approaches the elastic critical load $p^C = 1$ at $\tilde{k}_m = 1$, the denominator of equation (18) vanishes and $\tilde{\omega}_m$ approaches infinity.

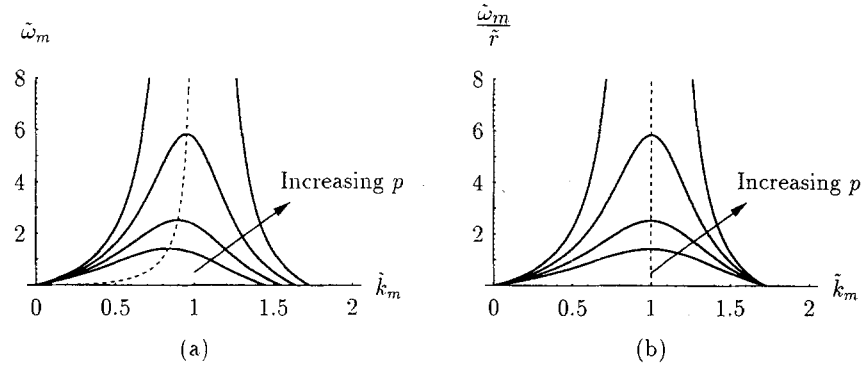

Figure 2
Nondimensional dispersion relations for a visco-elastic medium.

On the other hand, nondimensionalizing with respect to the dominant wavelength of the purely viscous system k_d by writing $\tilde{x} = k_d x$ and $\tilde{t} = \omega_d t$, where k_d and ω_d are given by equation (13), reduces equation (1) to,

$$\left(\dot{w}_m'''' + 3\dot{w}_m'' + \frac{2}{p^{3/2}} \tilde{k}_m \dot{w}_m \right) + \tilde{r}(w_m'''' + 3w_m'') = 0, \tag{19}$$

where $\tilde{r} = r/\omega_d$. The possibility of time-dependency in the spatial nondimensionalization apparently limits application to the case of constant load. Assuming again periodicity in x, with the eigensolution $a_m = A_m \, e^{\tilde{\omega}_m \tilde{t}}$, we obtain an alternative form for the visco-elsatic dispersion relation,

$$\tilde{\omega}_m = \frac{3\tilde{k}_m - \tilde{k}_m^3}{\frac{2}{p^{3/2}} - 3\tilde{k}_m + \tilde{k}_m^3} \tilde{r}, \tag{20}$$

giving the family of curves of Figure 2(b). Now, in contrast to the purely viscous bed under the same nondimensionalization, p enters parametrically. As p approaches the elastic critical load $p^C = 1$ at $\tilde{k}_m = 1$, the denominator is again seen to vanish and $\tilde{\omega}_m$ approaches infinity.

We note at this stage a useful interrelation between the dominant viscous and minimum-load elastic wavenumbers,

$$k_d = k_{\min} \sqrt{p}. \tag{21}$$

2.3.1 Aperiodicity and Linear Eigenvalues

For a linear or the following nonlinear system, when w is small equation (17) must be satisfied. If the assumption of periodicity is replaced by the more general complex representation $w_m = a_m \, e^{\lambda \tilde{x}}$, where $\lambda = \alpha + i\beta$, the characteristic equation,

$$\lambda^4 + 3p\lambda^2 + 2\tilde{k}_m = 0, \tag{22}$$

again imparts a zero denominator to (18). Substituting for λ and setting real and imaginary parts to zero results in the relations,

$$f_1 = \alpha^4 - 6\alpha^2\beta^2 + \beta^4 + 3p(\alpha^2 - \beta^2) + 2\tilde{k}_m = 0,$$
$$f_2 = 2\alpha\beta(2\alpha^2 + 3p - 2\beta^2) = 0, \tag{23}$$

representing allowable elastic solutions near the flat state $w = 0$. If we set $\alpha = 0$ and $\beta = \tilde{k}_m$, the periodic solutions of the previous section appear, but non-zero values of α can also satisfy these expressions—describing fluctuating forms with amplitudes that either grow or diminish exponentially, as in the tails of localized solutions. If α is small and the amplitude is slowly varying (HUNT *et al.*, 1989), it is then reasonable to assume that the wavelength of this linearized solution matches that of the bedding relation. In all that follows we thus shall be setting,

$$\beta = \tilde{k}_m. \tag{24}$$

The effect of the bedding relation is such that the *eigenvalues* α and β are more difficult to identify than their Winkler counterparts (HUNT and WADEE, 1991), but the principle remains the same; they are both expressible in terms of p. The forms f_1 (with $\tilde{k}_m = \beta$) and f_2 are central to the following nonlinear study, where for $t \neq 0$ they appear as non-zero functions of time.

3. *Nonlinear Analysis*

Two different forms of nonlinearity are to be considered. First, a softening cubic nonlinearity is introduced into the bedding relation (15), which in an associated elastic problem has the effect of inducing localized buckling (HUNT and WADEE, 1991; CHAMPNEYS and TOLAND, 1993). Secondly, in a quest for physical reality, we shall consider the evolution to be under conditions of constant end displacement. Displacement control under periodic conditions introduces a 'noncoupling' end-restraint nonlinearity (MÜHLHAUS, 1993; MÜHLHAUS *et al.*, 1994); when a constant axial displacement is prescribed at the plate edges, the driving force of the instability, the effective axial force, decreases during the fold evolution according to,

$$P_{\text{eff}} = P - \frac{Eh}{1 - \nu^2}(w')^2_{av}, \tag{25}$$

where,

$$(w')^2_{av} = \frac{1}{L}\int_0^L w'^2 \, \mathrm{d}x = \tfrac{1}{2}\sum_{m=0}^{\infty} k_m^2 a_m^2. \tag{26}$$

The combined effect of both nonlinearities is such that the Fourier representations of the previous section, familiar also from the work of BIOT (1965), no longer

fit the bill: the more localized a response, or alternatively the longer the specimen, the less well the displaced shape is modelled by a concoction of periodic modes. Instead, we start by assuming that a specified end-shortening Δ is suddenly imposed at time $t = 0$, and is thereafter maintained as constant. There is thus a clearly defined initial elastic phase, followed by a slow (viscous) evolution over time. An ordinary differential equation (ODE) is defined for the elastic phase, for which a valid solution appears in the form of a localized fluctuating buckle, modulated spatially in both amplitude and phase. Associated solutions of the governing nonlinear partial differential equation (PDE) of evolution are then sought. Rather than deal in dominant wavelengths (BIOT, 1965; MÜHLHAUS *et al.*, 1994), we observe how the continuous response of this equation changes in wavelength and in the modulations of both amplitude and phase, over time. The outcome is a convincing time history.

3.1 Softening Foundation and Localization

A cubic softening nonlinearity in the bedding relations alters the expected form of the response from periodic to localized. For a visco-elastic medium with a general cubic nonlinearity we can write the dimensional form of the governing nonlinear partial differential equation as,

$$\frac{Gh^3}{3}\partial_x^4 w + P\partial_x^2 w + 4G_1 k_m\left(\frac{\partial_t}{\partial_t + r}\right)(w + \zeta w^3) = 0, \tag{27}$$

where in general ζ can be positive or negative. The wavelength dependence of the bedding relation, expressed by k_m in the coefficient of the final term, is assumed to extend to the nonlinear term as shown. We are of course aware that this effect arises from purely linear considerations (BIOT, 1965), but retain it in the nonlinear term on the basis that, in the absence of further information, whether or not it is included will have little qualitative effect on the outcome. This is indeed confirmed by numerical experiment.

The governing nonlinear equation can also be written,

$$\partial_t\left[\frac{Gh^3}{3}\partial_x^4 w + P\partial_x^2 w + 4G_1 k_m(w + \zeta w^3)\right] + r\left(\frac{Gh^3}{3}\partial_x^4 w + P\partial_x^2 w\right) = 0. \tag{28}$$

With the earlier nondimensionalizations defined with respect to the elastic critical wavelength $k_{\min}$, and setting in addition $\tilde{w} = \sqrt{|\zeta|}w$, we write this as,

$$\partial_{\tilde{t}}[\tilde{w}'''' + 3p\tilde{w}'' + 2\tilde{k}_m(\tilde{w} \pm \tilde{w}^3)] + (\tilde{w}'''' + 3p\tilde{w}'') = 0, \tag{29}$$

where the $+$ sign represents a hardening foundation and the $-$ sign a softening foundation. These two cases must be considered separately. From this point we shall drop the tilde from all nondimensisonal representations and consider only the softening nonlinearity.

3.2 Initial Elastic Phase

The fundamental nonlinear differential equation becomes,

$$\partial_t[w'''' + 3pw'' + 2k_m(w - w^3)] + (w'''' + 3pw'') = 0, \tag{30}$$

and to explore the instantaneous elastic response we set the square brackets to zero,

$$w'''' + 3pw'' + 2k_m(w - w^3) = 0, \tag{31}$$

which is of course the equilibrium equation for a purely elastic embedding medium. All the machinery of elastic analysis is now available (see for example, HUNT and WADEE, 1991; HUNT *et al.*, 1993). The prospect of localized solutions, described by a homoclinic loop in phase space and for a long strut representing the most likely outcome in practice, must be considered. Close to the elastic critical point we thus look for solutions of the form,

$$w = A \operatorname{sech} \alpha x \cos \beta x + B \operatorname{sech} \alpha x \tanh \alpha x \sin \beta x. \tag{32}$$

This introduces the possibility of a modulation to the amplitude of a harmonic function, expressed by the sech function, together with a phase modulation determined by the relation between A and B. We note also that α and β are respectively the real and imaginary parts of the linearized solution of equation (31), as expressed by equations (23) which define respectively the rate of exponential growth/decay and the wavelength of the modulated periodicity at the tails of the localization; we henceforth match this with the wavelength of the bedding relation by setting $k_m = \beta$, as described above in equation (24).

After substituting into equation (31) and cancelling by sech αx, we obtain,

$$\begin{aligned}
&(f_1 A - f_2 B) \cos \beta x + (f_2 A + f_1 B) \tanh \alpha x \sin \beta x + [\alpha^2(12\beta^2 - 6p - 20\alpha^2)A \\
&\quad -4\alpha\beta(2\beta^2 - 3p - 20\alpha^2)B - \tfrac{3}{2}\beta A(A^2 + B^2)] \operatorname{sech}^2 \alpha x \cos \beta x \\
&\quad +[-24\alpha^3\beta A + 6\alpha^2(6\beta^2 - 3p - 10\alpha^2)B \\
&\quad -\tfrac{3}{2}\beta B(A^2 + B^2)] \operatorname{sech}^2 \alpha x \tanh \alpha x \sin \beta x + \cdots = 0,
\end{aligned} \tag{33}$$

where f_1 and f_2 are the same expressions as in equations (23), and $\cdots$ conceals (small) higher-order terms involving $\operatorname{sech}^4 \alpha x$, $\sin 3\beta x$ and $\cos 3\beta x$. Approximate solutions to the governing differential equation are obtained by setting the coefficient of $\cos \beta x$ and $\sin \beta x$ to zero. There are two distinct sets. First, putting $\alpha = 0$ implies that the solution is periodic. Phase shift can then be ignored as being merely a translation in x and so B can be set to zero. We then have the periodic form picked out by the linear visco-elastic dispersion relation (18) at $p = p^C = 1$, but extended into the nonlinear regime,

$$A^2 = \tfrac{2}{3}[\beta(\beta^2 - 3p) + 2]. \tag{34}$$

We note the existence of real solutions for $\beta = 1$ and $0 < p < 1$, describing subcritical periodic post-buckled states.

On the other hand, $\alpha \neq 0$ solutions appear if all four terms of equation (33) are simultaneously zero. The first two, coefficients purely of $\cos \beta x$ and $\sin \beta x$, are free from nonlinearity, and are satisfied by the complex linear eigenvalues of equations (23) for which $f_1 = f_2 = 0$; the assumed localized form thus matches the linearized solution for small w as expected. The remaining two terms set the amplitude and phase of the localized buckle pattern, expressed in the solution for A and B of the two nonlinear equations,

$$\alpha^2(12\beta^2 - 6p - 20\alpha^2)A - 4\alpha\beta(2\beta^2 - 3p - 20\alpha^2)B - \tfrac{3}{2}\beta A(A^2 + B^2) = 0,$$

$$-24\alpha^3\beta A + 6\alpha^2(6\beta^2 - 3p - 10\alpha^2)B - \tfrac{3}{2}\beta B(A^2 + B^2) = 0. \tag{35}$$

We note that if α is taken to be small and α^2 ignored in comparison with β^2, in conjunction with the linear eigenvalues of equations (23) this gives

$$B \simeq \frac{2\alpha\beta}{2\beta^2 - p} A, \tag{36}$$

and B is small in comparison with A.

Solutions to (35) are readily obtained numerically. Initially B can be assumed zero and the first equation solved for A, the obtained results then substituted into the second equation which is solved for B, both results substituted into the first equation to provide an improved result for A, and so on. The linear eigenvalue solution (23) shows that this collapses on to the flat fundamental state $A = B = 0$ at $\alpha = 0$, $\beta = 2^{1/3}$, $p = 2^{5/3}/3 \simeq 1.058$, just above the lowest elastic critical load at $\beta = 1$, $p^C = 1$; the latter thus admits only periodic buckling. However, for long

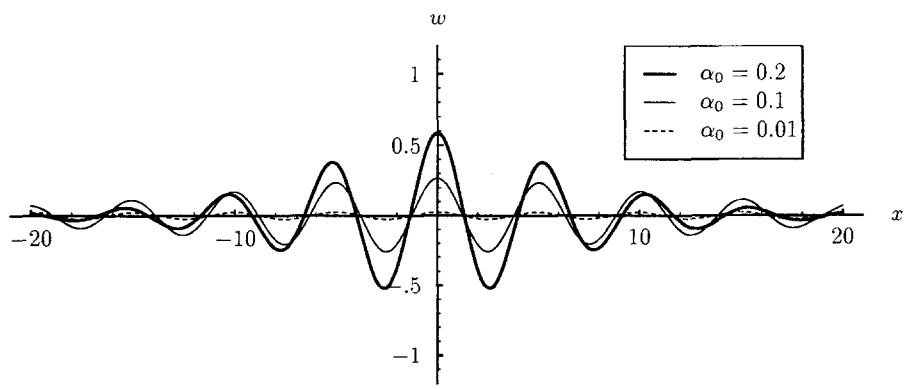

Figure 3
Three instantaneous elastic responses.

structures, the load to end-shortening response for localized behaviour has a more severe stability characteristic than its periodic counterpart (HUNT *et al.*, 1989), and localization becomes significant almost as soon as the post-buckling range is entered, despite the slightly higher critical load.

3.2.1 Initial End-shortening

Under constant load conditions all subcritical post-buckling states are unstable; this can be demonstrated either by elastic analysis at $t=0$ or evolution via the diffusion equations seen later. To stabilize the initial elastic phase we can constrain the end displacement. If the layer is assumed to be inextensional, the first-order nondimensional geometric end-shortening Δ due to the localized form (32) is,

$$\begin{aligned}\Delta &= \tfrac{1}{2}\int_{-\infty}^{\infty} (w')^2\,\mathrm{d}x \\ &= \tfrac{1}{4}\int_{-\infty}^{\infty} \{[(\alpha^2+\beta^2)(A^2+B^2)\,\mathrm{sech}^2\,\alpha x + 4\alpha^2B^2\,\mathrm{sech}^6\,\alpha x \\ &\quad -(\alpha^2A^2+4\alpha^2B^2+2\alpha\beta AB+\beta^2B^2)\,\mathrm{sech}^4\,\alpha x] \\ &\quad +[(\alpha^2A^2-\alpha^2B^2-4\alpha\beta AB-\beta^2A^2+\beta^2B^2)\,\mathrm{sech}^2\,\alpha x \\ &\quad -(\alpha^2A^2-4\alpha^2B^2-6\alpha\beta AB+\beta^2B^2)\,\mathrm{sech}^4\,\alpha x \\ &\quad -4\alpha^2B^2\,\mathrm{sech}^6\,\alpha x]\cos 2\beta x \\ &\quad +2[(\alpha\beta A^2-\alpha\beta B^2+\alpha^2AB-\beta^2AB)\,\mathrm{sech}^2\,\alpha x\tanh\alpha x \\ &\quad +2\alpha B(\beta B-\alpha A)\,\mathrm{sech}^4\,\alpha x\tanh\alpha x]\sin 2\beta x\}\,\mathrm{d}x. \end{aligned} \tag{37}$$

This is readily integrable if terms in $\cos 2\beta x$ and $\sin 2\beta x$ are ignored. These can be shown to vanish as $\alpha\to 0$ by repeatedly integrating by parts (HUNT and WADEE, 1991), and introduce small errors for small but non-zero values of α; they are obtainable via so-called contour integrals (GRADSHTEYN and RYZHIK, 1994), but would introduce extra complexities to the analysis that follows. In Section 3.5 we check end-shortening by integrating numerically in x, to give some account of the errors introduced by this and other approximations.

Evaluation of the remaining integrals in (37) then leaves,

$$\Delta = \frac{1}{30\alpha}[5(3\beta^2+\alpha^2)A^2 - 20\alpha\beta AB + (5\beta^2+7\alpha^2)B^2]. \tag{38}$$

To reduce the possibility of error, these expressions have been produced using the algebraic manipulation package Mathematica (WOLFRAM, 1988). Several allowable elastic solutions for a range of initial α_0 values are shown in Figure 3. We note the general trend that the greater the chosen value of α_0, the greater the initial end-shortening, the more localized the elastic response, and the lower the initial load.

3.3 Time Evolution

The significance of the localized form at the start of the evolutionary process is that, in contrast with the purely viscous foundation (BIOT, 1965), $t \neq 0$ solutions display more than just the growth of periodic amplitudes. Decay of localization into a final homogeneous state must also be considered. If the layer is infinitely long, end-shortening of a finite-amplitude periodic buckle is similarly infinite, but end-shortening of a localized buckle is finite. For long systems under constant or slowly-varying applied end displacement, it is therefore useful to envisage decay of an initial localized state through a succession of localized states to the end result of a nearly-flat state, in the complete absence of periodicity.

The procedure for following the evolution takes much the same course with equation (30) as the elastic analysis with equation (31). An assumed form for the deflected shape is substituted into the governing differential equation and coefficients of the lower-order contributions, sech $\alpha x \cos \beta x$, etc., set to zero. Now however, because α and β are free to vary in time, terms in x sech $\alpha x \sin \beta x$ and x sech $\alpha x \tanh \alpha x \cos \beta x$ start to appear, and to account successfully for these during evolution, similar forms are introduced into the assumed expression for w, giving the primitive form,

$$w = A \operatorname{sech} \alpha x \cos \beta x + B \operatorname{sech} \alpha x \tanh \alpha x \sin \beta x + Cx \operatorname{sech} \alpha x \sin \beta x + Dx \operatorname{sech} \alpha x \tanh \alpha x \cos \beta x. \quad (39)$$

The inclusion of terms in x implies that after differentiation with respect to time, terms in x^2 appear, which themselves should then be included in the initial form, and so on. The following formulation is limited to the four terms of (39), on the basis that such effects are increasingly of higher and higher order. The difference between the evolution with just A and B, and with A, B, C and D, is explored in Section 3.4.

With A, B, C, D, α, β and p as unknown variables in t, we then look to reduce the nonlinear PDE (30) to seven simultaneous first-order ODEs. Six of these equations result from setting specific coefficients to zero, as described below and seen in detail in the Appendix; the seventh comes from the constraint of constant end-shortening.

3.3.1 Constant End-shortening

As before, total end-shortening is given by the integral $\Delta = \frac{1}{2}\int_{-\infty}^{\infty}(w')^2\,dx$. After substituting the above expression for w, if terms in $\sin 2\beta x$ and $\cos 2\beta x$ are ignored as before, all integrations can be carried out within Mathematica. This gives,

$$\begin{aligned}\Delta = {} & \left(\frac{\beta^2}{2\alpha} + \frac{\alpha}{6}\right)A^2 - \frac{2\beta}{3}AB + \left(\frac{\beta^2}{6\alpha} + \frac{7\alpha}{30}\right)B^2 - \frac{\beta}{\alpha}AC \\ & + \left(\frac{\beta^2}{2\alpha^2} + \frac{1}{2}\right)BC + \left(\frac{\pi^2\beta^2}{24\alpha^3} + \frac{\pi^2+12}{72\alpha}\right)C^2 + \left(\frac{\beta^2}{2\alpha^2} - \frac{1}{6}\right)AD \\ & + \frac{\beta}{3\alpha}BD + \frac{\beta}{3\alpha^2}\left(\frac{\pi^2}{6} - 1\right)CD + \left(\frac{\beta^2(\pi^2+12)}{72\alpha^3} + \frac{7\pi^2}{360\alpha}\right)D^2, \end{aligned} \quad (40)$$

and differentiating with respect to t,

$$\frac{\partial \Delta}{\partial \alpha}\dot{\alpha} + \frac{\partial \Delta}{\partial \beta}\dot{\beta} + \frac{\partial \Delta}{\partial A}\dot{A} + \frac{\partial \Delta}{\partial B}\dot{B} + \frac{\partial \Delta}{\partial C}\dot{C} + \frac{\partial \Delta}{\partial D}\dot{D} = 0. \tag{41}$$

Coefficients $\partial\Delta/\partial\alpha$ etc. of this first-order equation in t, representing the constraint of constant end-shortening, are readily found and are given in the Appendix.

3.3.2 Remaining Diffusion Equations

Seven unknown variables and a single constraint equation suggest that six further equations in time should lead to a well-posed problem. If the required differentiations are performed on equation (39) and the result substituted into the fundamental partial differential equation (30), complicated expressions are to be expected. Now however, with the power of modern algebraic manipulation packages, this task can be reduced to a simple algorithm, which with careful programming can be relied upon as being error-free.

We can thus set the coefficients of $\operatorname{sech} \alpha x \cos \beta x$, $\operatorname{sech} \alpha x \tanh \alpha x \sin \beta x$, $\operatorname{sech}^3 \alpha x \cos \beta x$, $\operatorname{sech}^3 \alpha x \tanh \alpha x \sin \beta x$, $x \operatorname{sech} \alpha x \sin \beta x$, and $x \operatorname{sech} \alpha x \tanh \alpha x \cos \beta x$, to zero to provide the extra six equations. All differentiations and collection of like terms can be performed within Mathematica, giving the coefficients found in the Appendix; they have also been output into C-format (WOLFRAM, 1988) and introduced directly into a program written in the computer language "C" to form the evolutionary time plots seen later in Section 3.4.

3.3.3 Initial Conditions

At the start of the evolutionary process, initial conditions are set by the elastic phase, which for a particular end-shortening Δ furnishes initial values α_0, β_0, p_0, A_0 and B_0, along with $C_0 = D_0 = 0$ for the remaining two unknowns. With the full seven variables however, a significant difficulty is encountered at the start of the evolutionary process; each of the final two equations of the Appendix, relating to coefficients of $x \operatorname{sech} \alpha x \sin \beta x$, and $x \operatorname{sech} \alpha x \tanh \alpha x \cos \beta x$, has a full set of zero coefficients at $t = 0$. We are therefore left with a double singularity at the start—five equations expressing seven unknowns. Since this is only an initial (startup) problem, it can usefully be seen as a shortage of a couple of initial conditions; after the start the missing two equations cut in, and the scheme progresses smoothly in the full seven variables.

We believe this problem to be an inevitable consequence of the visco-elasticity, with its two disassociated time scales. The "instantaneous" response described by the initial elastic phase would of course involve inertial effects not included here, but which in the evolutionary time scale would provide a set of initial velocities. It is apparently a limitation of the present formulation that all starting conditions cannot be completely specified; certain "initial transients" remain undefined. There is no obvious cure for the chosen constituent model of the foundation. Only by slowing down the instantaneous response could we be sure of the validity of

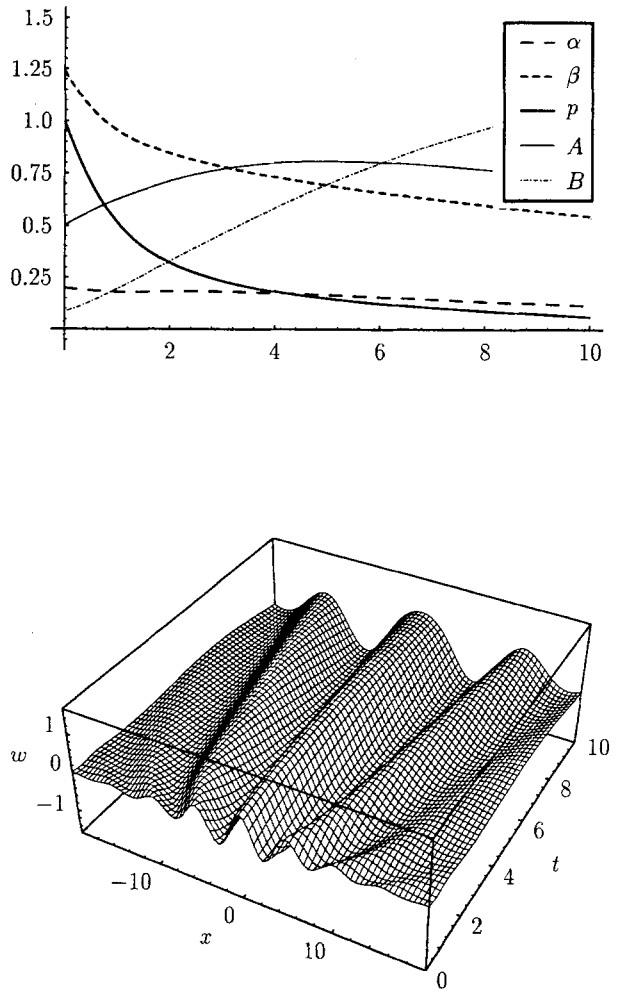

Figure 4
Five variable evolution with $\alpha_0 = 0.2$, $\Delta t = 0.01$.

ignoring inertial effects. This could be achieved by replacing the Maxwell fluid by a three parameter fluid based on a Kelvin/Voigt solid in series with a dashpot, a promising development that is yet to be explored.

3.4 Results

The process for following the time evolutions is as follows. An initial value of α_0 is first chosen, from which end-shortening Δ and the initial (elastic) response are determined as prescribed above. The first-order equations of the Appendix are then integrated forward in time, using a forward-difference technique with a small

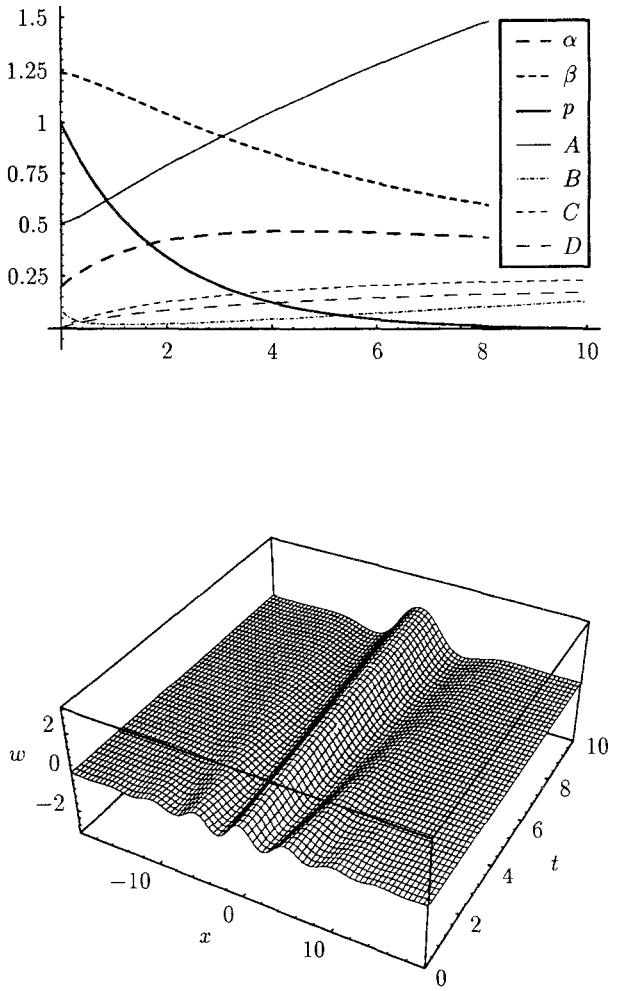

Figure 5
Seven variable evolution with $\alpha_0 = 0.2$, $\Lambda = 0.01$, $\dot{\beta}_0 = 0$, $\dot{C}_0 = 0.18$.

increment, typically $\Delta t = 0.01$. Figure 4 shows a typical response if C and D are suppressed and only five equations used. Figure 5 shows the comparable result when C and D are allowed to vary and all seven equations are used. There is no problem with an initial singularity for Figure 4, but Figure 5 is subject to two extra (assumed) initial conditions as described above and explored further as follows.

Figure 6 compares two possible sets of initial conditions over short- and long-term evolution, the top diagrams being for $\dot{\beta}_0 = 0$, $\dot{C}_0 = 0.18$, and the bottom two for $\dot{C}_0 = \dot{D}_0 = 0$; the latter corresponds to the five-variable evolution of Figure 4 for the first time step alone, followed by seven-variable evolution. Small differ-

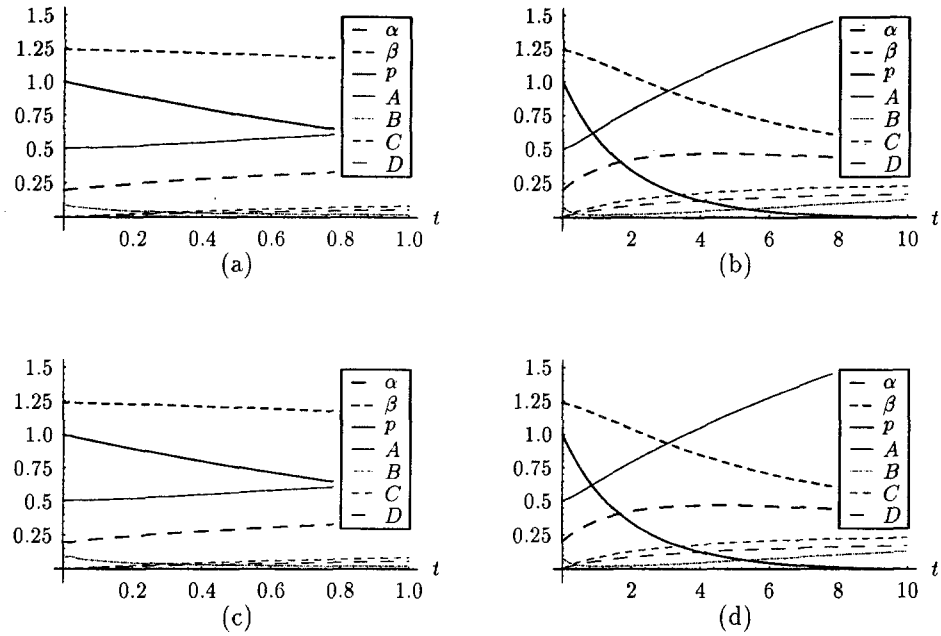

Figure 6
Seven variable evolution with different initial conditions: $\alpha_0 = 0.2$, $\Delta t = 0.01$. Top: $\dot{\beta}_0 = 0$, $\dot{C}_0 = 0.18$. Bottom: $\dot{C}_0 = \dot{D}_0 = 0$.

ences can be detected at the start, as might be expected, but the long-term evolutionary patterns are broadly similar; other starting conditions tested also led to similar initial perturbations, either to a greater or lesser extent, as those seen in Figure 6(c), but again the subsequent evolution is always broadly like that of Figure 5. All contrast sharply with Figure 4 however, which is clearly experiencing a greater degree of constraint over time.

This point is reinforced in Figure 7, which compares long, and very long, term evolution for five and seven variable formulations. The five variable evolution, at the top, is seen to experience considerably greater disturbance than the seven variable evolution at the bottom; C and D are clearly having a smoothing effect. A time sequence of successive sections through Figure 7(c) is also shown in Figure 8.

It is interesting to observe qualitatively the sequence of events for this nondimensionalized and hence quite general treatment. The first and most significant feature is that the load drops quickly to zero as the viscous part of the foundation absorbs its stored energy. In common with the elastic response (CHAMPNEYS and TOLAND, 1993), the lower the load the more localized the form, and so the drop in load is accompanied by an increase in α. In the meantime, β also tends to fall, indicating an increase in wavelength as the elastic bending energy in the layer is released. The combined effect is to evolve towards the single long wave

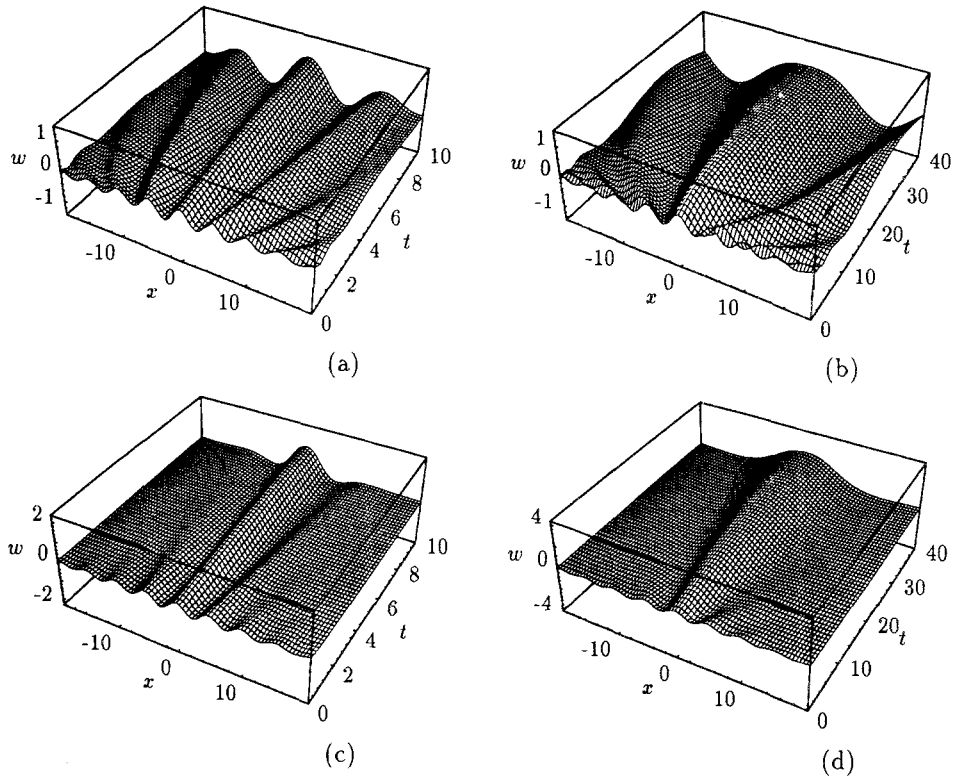

Figure 7
Five and seven variable comparison: $\alpha_0 = 0.1$. $\Delta t = 0.01$. Top: $C = D = 0$ for all time. Bottom: seven variable evolution with $\beta_0 = 0$, $C_0 = 0.086$.

without ever approaching a periodic form. We note again that localization is by its very nature nonlinear, and the analysis thus has a quite different flavour from the linear, periodic, contributions of BIOT (1965).

At the time limit of the evolutionary process there is a tendency for the load p to take small negative values. We attribute this unlikely event to approximations inherent in the analysis, as discussed below.

3.5 Approximations

There are three different types of approximation in the above formulation that we can identify as likely to affect the accuracy of the results over time. The first is the assumption of a finite number of modeforms in equation (39). Just as terms described by A and B imply the presence of small contributions C and D as time progresses, so do the latter imply yet smaller terms in x^2, which in turn imply terms

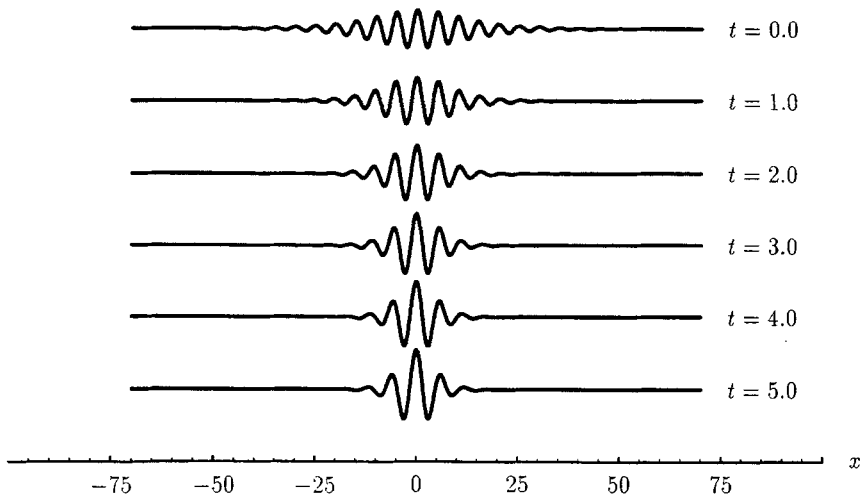

Figure 8
Sections through Figure 7(c) at constant t.

in x^3 and so on. The differences in the evolutions of Figure 7 give some indication of the significance of this effect.

A second type of approximation follows from the assumption that α is small. Among such effects we might include the higher-order terms in $\text{sech}^4\,\alpha x$ that are ignored after substitution into the governing partial differential equation, and terms in $\sin 2\beta x$ and $\cos 2\beta x$ in the integrand (37) of the end-shortening. We see from Figures 4 and 5 that, even if the initial α_0 is small, α grows to a maximum value of about 0.4 before falling. Such higher-order effects are likely to be significant by this stage of the evolution.

Finally there are approximations deriving from the inherent assumption that deflections, although moderately large, are not gross. Terms in $\sin 3\beta x$ and $\cos 3\beta x$ that are ignored after substitution into the governing equation are of this nature; unlike the above, they would affect results that are purely periodic. Other higher-order terms in $(w')^4$, $(w')^6$, etc. that nominally should appear in the full integrand for end-shortening (THOMPSON and HUNT, 1973), are likewise ignored; these are the same as the so-called "elastica" large-deflection terms (HUNT *et al.*, 1993), and to include them would therefore demand, for consistency, extensive modifications to the governing differential equations.

Much of the above could be addressed with the addition of extra modeforms to (39), although the spatially-chaotic nature of the related elastic system does suggest that the problems can never be overcome completely (HUNT and WADEE, 1991; CHAMPNEYS and TOLAND, 1993). A check on the approximations associated with the end-shortening is provided by the following reasoning.

Although not included analytically, the effects of ignoring certain integrals in the evaluation of the end-shortening (40) can at least be estimated. The actual

end-shortening of the numerical model can be evaluated by summing $\Delta = \Sigma\,(1 - \sqrt{1 - w'^2})\,\delta x$ over the range of x for which w is computationally finite; this can then be compared with the assumed Δ from equation (38). For the initial elastic phase, at $\alpha_0 = 0.1$ a difference of about 2% is found. Binomial expansion of the above summation, for which the first term is $\frac{1}{2}\Sigma\,(w')^2\,\delta x$, shows that the difference is almost entirely due to the higher-order terms in $(w')^4$, $(w')^6$. etc., which remain outside the scope of this formulation (see above); for this small value of α the missing contribution from the contour integrals is thus negligible. In the time it takes for the load to fall to zero the disparity grows to about 12%; similar breakdown by binomial expansion attributes about half of this to the higher terms, and about half to the contour integrals, which we would expect to have a growing influence as α increases.

It must be emphasized however that this can only be a rough guide to the effects of the missing terms. Their true significance will only be revealed when the complete, exact, response is known.

4. *Concluding Remarks*

We regard this paper mostly as a pilot study. Questions remain unanswered, for example the relative significance of the approximations discussed above. Its importance however is that it provides a mechanism, possibly for the first time, for aperiodicity and localization to govern within the geological framework. There are a number of developments that are thus worthy of further examination.

It may for example be asked just how a particular physical system will set about selecting its initial end-shortening. The answer lies in extra effects not included here. The first is axial compressibility, which is relatively simple to include, and gives to the load to end-shortening (effective stiffness) relation a characteristic "C" shape, seen for example in the application of elastic localization theory to uplift buckling in pipelines (BLACKMORE and HUNT, 1996). A second effect is that of imperfections, nontrivial to handle, which can round off subcritical bifurcations at loads only a fraction of the lowest classical critical (linear eigenvalue) result. The combined effect is for the elastic system to snap-buckle at some load determined by imperfection shape and magnitude, at an end-shortening initially comprising mainly axial compression. The subsequent sudden release in load signifies axial compression giving way to geometric end-shortening of the kind considered here. Full treatment, including imperfection effects, is marked for future study.

It is also perhaps lacking a certain realism to propose that any event of geological folding would occur instantly, as suggested by this model employing a Maxwell fluid for the bedding material. The model does emphasize, however, that two quite different time scales may be involved, one in which the response is *predominately* elastic and localization may develop, and one in which viscous

dispersion is the governing effect and it evolves. It may be more realistic to see both effects in the same timeframe, which should be achievable by replacing the Maxwell foundation by a three parameter fluid comprising a Kelvin/Voigt unit in series with a dashpot. The folding mechanism seen here—instantaneous localization followed by slow diffusion—would then given way to a family of possible evolutionary histories in a single t, with the particular pattern depending on the various parameters of the formulation. Again with the help of Mathematica it is hoped that this will prove to be a relatively straightforward operation.

Acknowledgments

The authors would like to acknowledge the support of Bruce Hobbs, without whom this work would not have arisen, and Bruce and Alison Ord for helpful discussions. Financial support for A. Whiting is provided by the Sir Robert Menzies Memorial Trust.

Appendix

Components of $\mathbf{M}\dot{\mathbf{q}} = \mathbf{r}$ *where* $\dot{\mathbf{q}} = [\dot{\alpha}, \dot{\beta}, \dot{p}, \dot{A}, \dot{B}, \dot{C}, \dot{D}]^T$

constant end-shortening:

$$\mathbf{M}_{11} = \frac{A^2}{6} - \frac{\beta^2 A^2}{2\alpha^2} + \frac{7B^2}{30} - \frac{\beta^2 B^2}{6\alpha^2} + \frac{\beta AC}{\alpha^2} - \frac{\beta^2 BC}{\alpha^3} - \frac{C^2}{6\alpha^2} - \frac{\pi^2 C^2}{72\alpha^2} - \frac{\pi^2\beta^2 C^2}{8\alpha^4} - \frac{\beta^2 AD}{\alpha^3} - \frac{\beta BD}{3\alpha^2} + \frac{2\beta CD}{3\alpha^3} - \frac{\pi^2\beta CD}{9\alpha^3} - \frac{7\pi^2 D^2}{360\alpha^2} - \frac{\beta^2 D^2}{2\alpha^4} - \frac{\pi^2\beta^2 D^2}{24\alpha^4},$$

$$\mathbf{M}_{12} = \frac{\beta A^2}{\alpha} - \frac{2AB}{3} + \frac{\beta B^2}{3\alpha} - \frac{AC}{\alpha} + \frac{\beta BC}{\alpha^2} + \frac{\pi^2\beta C^2}{12\alpha^3} + \frac{\beta AD}{\alpha^2} + \frac{BD}{3\alpha} - \frac{CD}{3\alpha^2} + \frac{\pi^2 CD}{18\alpha^2} + \frac{\beta D^2}{3\alpha^3} + \frac{\pi^2\beta D^2}{36\alpha^3},$$

$$\mathbf{M}_{13} = 0,$$

$$\mathbf{M}_{14} = \frac{\alpha A}{3} + \frac{\beta^2 A}{\alpha} - \frac{2\beta B}{3} - \frac{\beta C}{\alpha} - \frac{D}{6} + \frac{\beta^2 D}{2\alpha^2},$$

$$\mathbf{M}_{15} = \frac{-2\beta A}{3} + \frac{7\alpha B}{15} + \frac{\beta^2 B}{3\alpha} + \frac{C}{2} + \frac{\beta^2 C}{2\alpha^2} + \frac{\beta D}{3\alpha},$$

$$\mathbf{M}_{16} = \frac{-\beta A}{\alpha} + \frac{B}{2} + \frac{\beta^2 B}{2\alpha^2} + \frac{C}{3\alpha} + \frac{\pi^2 C}{36\alpha} + \frac{\pi^2\beta^2 C}{12\alpha^3} - \frac{\beta D}{3\alpha^2} + \frac{\pi^2\beta D}{18\alpha^2},$$

$$\mathbf{M}_{17} = \frac{-A}{6} + \frac{\beta^2 A}{2\alpha^2} + \frac{\beta B}{3\alpha} - \frac{\beta C}{3\alpha^2} + \frac{\pi^2\beta C}{18\alpha^2} + \frac{7\pi^2 D}{180\alpha} + \frac{\beta^2 D}{3\alpha^3} + \frac{\pi^2\beta^2 D}{36\alpha^3},$$

$$\mathbf{r}_1 = 0.$$

coefficient of sech $\alpha x \cos \beta x$:

$$\begin{aligned}
\mathbf{M}_{21} &= 4\alpha^3 A - 12\alpha\beta^2 A + 6\alpha p A - 12\alpha^2\beta B + 4\beta^3 B - 6\beta p B \\
&\quad + 24\alpha\beta C - 12\alpha^2 D + 12\beta^2 D - 6pD, \\
\mathbf{M}_{22} &= 2A - 12\alpha^2\beta A + 4\beta^3 A - 6\beta p A - 4\alpha^3 B + 12\alpha\beta^2 B \\
&\quad - 6\alpha p B + 12\alpha^2 C - 12\beta^2 C + 6pC + 24\alpha\beta D, \\
\mathbf{M}_{23} &= 3\alpha^2 A - 3\beta^2 A - 6\alpha\beta B + 6\beta C - 6\alpha D, \\
\mathbf{M}_{24} &= \alpha^4 + 2\beta - 6\alpha^2\beta^2 + \beta^4 + 3\alpha^2 p - 3\beta^2 p, \\
\mathbf{M}_{25} &= -4\alpha^3\beta + 4\alpha\beta^3 - 6\alpha\beta p, \\
\mathbf{M}_{26} &= 12\alpha^2\beta - 4\beta^3 + 6\beta p, \\
\mathbf{M}_{27} &= -4\alpha^3 + 12\alpha\beta^2 - 6\alpha p, \\
r_2 &= -\alpha^4 A + 6\alpha^2\beta^2 A - \beta^4 A - 3\alpha^2 p A + 3\beta^2 p A + 4\alpha^3\beta B \\
&\quad - 4\alpha\beta^3 B + 6\alpha\beta p B - 12\alpha^2\beta C + 4\beta^3 C - 6\beta p C + 4\alpha^3 D \\
&\quad - 12\alpha\beta^2 D + 6\alpha p D.
\end{aligned}$$

coefficient of sech $\alpha x \tanh \alpha x \sin \beta x$:

$$\begin{aligned}
\mathbf{M}_{31} &= 12\alpha^2\beta A - 4\beta^3 A + 6\beta p A + 4\alpha^3 B - 12\alpha\beta^2 B + 6\alpha p B \\
&\quad - 12\alpha^2 C + 12\beta^2 C - 6pC - 24\alpha\beta D, \\
\mathbf{M}_{32} &= 4\alpha^3 A - 12\alpha\beta^2 A + 6\alpha p A + 2B - 12\alpha^2\beta B + 4\beta^3 B \\
&\quad - 6\beta p B + 24\alpha\beta C - 12\alpha^2 D + 12\beta^2 D - 6pD, \\
\mathbf{M}_{33} &= 6\alpha\beta A + 3\alpha^2 B - 3\beta^2 B - 6\alpha C - 6\beta D, \\
\mathbf{M}_{34} &= 4\alpha^3\beta - 4\alpha\beta^3 + 6\alpha\beta p, \\
\mathbf{M}_{35} &= \alpha^4 + 2\beta - 6\alpha^2\beta^2 + \beta^4 + 3\alpha^2 p - 3\beta^2 p, \\
\mathbf{M}_{36} &= -4\alpha^3 + 12\alpha\beta^2 - 6\alpha p, \\
\mathbf{M}_{37} &= -12\alpha^2\beta + 4\beta^3 - 6\beta p, \\
\mathbf{r}_3 &= -4\alpha^3\beta A + 4\alpha\beta^3 A - 6\alpha\beta p A - \alpha^4 B + 6\alpha^2\beta^2 B - \beta^4 B \\
&\quad - 3\alpha^2 p B + 3\beta^2 p B + 4\alpha^3 C - 12\alpha\beta^2 C + 6\alpha p C + 12\alpha^2\beta D \\
&\quad - 4\beta^3 D + 6\beta p D.
\end{aligned}$$

coefficient of $\operatorname{sech}^3 \alpha x \cos \beta x$:

$$\mathbf{M}_{41} = -80\alpha^3 A + 24\alpha\beta^2 A - 12\alpha p A + 240\alpha^2\beta B - 8\beta^3 B + 12\beta p B$$
$$-48\alpha\beta C + 240\alpha^2 D - 24\beta^2 D + 12pD,$$
$$\mathbf{M}_{42} = 24\alpha^2\beta A - \frac{3A^3}{2} + 80\alpha^3 B - 24\alpha\beta^2 B + 12\alpha p B - \frac{3AB^2}{2}$$
$$-24\alpha^2 C - 48\alpha\beta D,$$
$$\mathbf{M}_{43} = -6\alpha^2 A + 12\alpha\beta B + 12\alpha D,$$
$$\mathbf{M}_{44} = -20\alpha^4 + 12\alpha^2\beta^2 - 6\alpha^2 p - \frac{9\beta A^2}{2} - \frac{3\beta B^2}{2},$$
$$\mathbf{M}_{45} = 80\alpha^3\beta - 8\alpha\beta^3 + 12\alpha\beta p - 3\beta AB,$$
$$\mathbf{M}_{46} = -24\alpha^2\beta,$$
$$\mathbf{M}_{47} = 80\alpha^3 - 24\alpha\beta^2 + 12\alpha p,$$
$$\mathbf{r}_4 = 20\alpha^4 A - 12\alpha^2\beta^2 A + 6\alpha^2 p A - 80\alpha^3\beta B + 8\alpha\beta^3 B - 12\alpha\beta p B$$
$$+24\alpha^2\beta C - 80\alpha^3 D + 24\alpha\beta^2 D - 12\alpha p D.$$

coefficient of $\operatorname{sech}^3 \alpha x \tanh \alpha x \sin \beta x$:

$$\mathbf{M}_{51} = -72\alpha^2\beta A - 240\alpha^3 B + 72\alpha\beta^2 B - 36\alpha p B + 72\alpha^2 C + 144\alpha\beta D,$$
$$\mathbf{M}_{52} = -24\alpha^3 A + 72\alpha^2\beta B - \frac{3A^2 B}{2} - \frac{3B^3}{2} + 72\alpha^2 D,$$
$$\mathbf{M}_{53} = -18\alpha^2 B,$$
$$\mathbf{M}_{54} = -24\alpha^3\beta - 3\beta AB,$$
$$\mathbf{M}_{55} = -60\alpha^4 + 36\alpha^2\beta^2 - 18\alpha^2 p - \frac{3\beta A^2}{2} - \frac{9\beta B^2}{2},$$
$$\mathbf{M}_{56} = 24\alpha^3,$$
$$\mathbf{M}_{57} = 72\alpha^2\beta,$$
$$\mathbf{r}_5 = 24\alpha^3\beta A + 60\alpha^4 B - 36\alpha^2\beta^2 B + 18\alpha^2 p B - 24\alpha^3 C - 72\alpha^2\beta D.$$

coefficient of $x \operatorname{sech} \alpha x \sin \beta x$:

$$\mathbf{M}_{61} = -4\alpha^3\beta A + 4\alpha\beta^3 A - 6\alpha\beta p A - \alpha^4 B - 2\beta B + 6\alpha^2\beta^2 B$$
$$-\beta^4 B - 3\alpha^2 p B + 3\beta^2 p B + 8\alpha^3 C - 24\alpha\beta^2 C + 12\alpha p C$$
$$+24\alpha^2\beta D - 8\beta^3 D + 12\beta p D,$$

$$\mathbf{M}_{62} = -\alpha^4 A - 2\beta A + 6\alpha^2\beta^2 A - \beta^4 A - 3\alpha^2 pA + 3\beta^2 pA + 4\alpha^3\beta B - 4\alpha\beta^3 B + 6\alpha\beta pB + 2C - 24\alpha^2\beta C + 8\beta^3 C - 12\beta pC + 8\alpha^3 D - 24\alpha\beta^2 D + 12\alpha pD,$$

$$\mathbf{M}_{63} = 3\alpha^2 C - 3\beta^2 C + 6\alpha\beta D,$$

$$\mathbf{M}_{64} = 0,$$

$$\mathbf{M}_{65} = 0,$$

$$\mathbf{M}_{66} = \alpha^4 + 2\beta - 6\alpha^2\beta^2 + \beta^4 + 3\alpha^2 p - 3\beta^2 p,$$

$$\mathbf{M}_{67} = 4\alpha^3\beta - 4\alpha\beta^3 + 6\alpha\beta p,$$

$$\mathbf{r}_6 = -\alpha^4 C + 6\alpha^2\beta^2 C - \beta^4 C - 3\alpha^2 pC + 3\beta^2 pC - 4\alpha^3\beta D + 4\alpha\beta^3 D - 6\alpha\beta pD.$$

coefficients of x sech αx tanh αx cos βx:

$$\mathbf{M}_{71} = -\alpha^4 A - 2\beta A + 6\alpha^2\beta^2 A - \beta^4 A - 3\alpha^2 pA + 3\beta^2 pA + 4\alpha^3\beta B - 4\alpha\beta^3 B + 6\alpha\beta pB - 24\alpha^2\beta C + 8\beta^3 C - 12\beta pC + 8\alpha^3 D - 24\alpha\beta^2 D + 12\alpha pD,$$

$$\mathbf{M}_{72} = 4\alpha^3\beta A - 4\alpha\beta^3 A + 6\alpha\beta pA + \alpha^4 B + 2\beta B - 6\alpha^2\beta^2 B + \beta^4 B + 3\alpha^2 pB - 3\beta^2 pB - 8\alpha^3 C + 24\alpha\beta^2 C - 12\alpha pC + 2D - 24\alpha^2\beta D + 8\beta^3 D - 12\beta pD,$$

$$\mathbf{M}_{73} = -6\alpha\beta C + 3\alpha^2 D - 3\beta^2 D,$$

$$\mathbf{M}_{74} = 0,$$

$$\mathbf{M}_{75} = 0,$$

$$\mathbf{M}_{76} = -4\alpha^3\beta + 4\alpha\beta^3 - 6\alpha\beta p,$$

$$\mathbf{M}_{77} = \alpha^4 + 2\beta - 6\alpha^2\beta^2 + \beta^4 + 3\alpha^2 p - 3\beta^2 p,$$

$$\mathbf{r}_7 = 4\alpha^3\beta C - 4\alpha\beta^3 C + 6\alpha\beta pC - \alpha^4 D + 6\alpha^2\beta^2 D - \beta^4 D - 3\alpha^2 pD + 3\beta^2 pD.$$

References

BIOT, M. A. (1965), *Mechanics of Incremental Deformation* (Wiley, New York 1965).

BLACKMORE, A., and HUNT, G. W. (1996), *The Dynamical Phase-space Analogy as a Tool for the Analysis of Upheaval Buckling*, to be published.

CHAMPNEYS, A. R., and TOLAND, J. F. (1993), *Bifurcation of a Plethora of Large Amplitude Homoclinic Orbits for Hamiltonian Systems*, Nonlinearity *6*, 665–721.

GRADSHTEYN, I. S., and RYZHIK, I. M. (1994), In *Table of Integrals, Series and Products* (Jeffrey, A., ed.), 5th edn. (Harcourt Brace and Co. London), Translated from the Russian by Scripta Technica, Inc.

HUNT, G. W., and WADEE, M. K. (1991), *Comparative Lagrangian Formulations for Localized Buckling*, Proc. R. Soc. London. *A434*, 485–502.

HUNT, G. W., BOLT, H. M., and THOMPSON, J. M. T. (1989), *Structural Localization Phenomena and the Dynamical Phase-space Analogy*, Proc. R. Soc. Lond. *A425*, 245–267.

HUNT, G. W., WADEE, M. K., and SHIACOLAS, N. (1993), *Localized Elasticae for the Strut on the Linear Foundation*, A.S.M.E. J. Appl. Mech. *60*, 1033–1038.

MÜHLHAUS, H-B., *Evolution of elastic folds in plane strain.* In *Modern Approaches to Plasticity* (Kolymbas, D., ed.) (Elsevier, Amsterdam 1993) pp. 734–765.

MÜHLHAUS, H-B., HOBBS, B. E., and ORD, A., *The Role of Exial Constraints on the Evolution of Folds in Single Layers, Computer Methods and Advances in Geomechanics*, vol. 1 (Siriwardane, H. J., and Zaman, M. M., eds.) (A. A. Balkema, Rotterdam 1994) pp. 223–231.

PRICE, N. J., and COSGROVE, J. W., *Analysis of Geological Structures* (Cambridge University Press, Cambridge 1990).

THOMPSON, J. M. T., and HUNT, G. W., *A General Theory of Elastic Stability* (Wiley, London 1973).

WOLFRAM, S., *Mathematica: A System for Doing Mathematics by Computer*, 1st edn. (Addison-Wesley Publishing Company, Reading, Mass. 1988).

(Received May 17, 1995, accepted August 28, 1995)